



# The Open Construction and Building Technology Journal

Content list available at: [www.benthamopen.com/TOBCTJ/](http://www.benthamopen.com/TOBCTJ/)

DOI: 10.2174/1874836801610010274



## The Effect of Boundary Conditions on the Behaviour of Pointed Masonry Barrel Vaults: Late Gothic Cases in Scotland

D. Theodossopoulos\*, N. Makoond and L. AKL

*Architectural Technology and Conservation, Edinburgh School of Architecture and Landscape Architecture, University of Edinburgh, 20 Chambers Street, Edinburgh, UK*

Received: January 15, 2015

Revised: May 15, 2015

Accepted: July 9, 2015

**Abstract:** Barrel vaults provide effective fire-proof roofing in historic churches, castles, cloisters or halls that look for simple and utilitarian aesthetics, as long as they are strongly connected to sturdy lateral walls and transverse gables, conditions that limit their possibilities for spatial expression. A study of the effect of these conditions was carried out on the pointed vaults of a characteristic group of 15<sup>th</sup> century Scottish churches. Following earlier measured surveys that showed remarkable geometric integrity, 1/15-scale models of a representative form were made in reinforced plaster that could delay the cracks propagation enough to be monitored. Only the shell was considered, leaving the effect of ribs or diaphragms that hold the heavy flagstone roof for further study. The model was subject to symmetric and asymmetric horizontal spread, which simulated the insufficient containment of not very stiff walls, but included the effect of gable end walls. Cracks formed invariably at an early stage (3% of the span spread), propagating more rapidly and causing early failure at a symmetrical spread (15% of span), while the asymmetrical spread produced diagonal crack patterns across the vault at 33% of the span. Gables provided more stiff areas but eventually caused local detachment at the spread point, at only 5% of the span, with cracks propagating to the back wall and at a higher rate when a less stiff gable was included (13% of span). The results validated an FE model that provided further insight to the performance of the type at displacement and settlement, as exemplified in the case of Bothwell church in Scotland.

**Keywords:** Barrel vaults, Experiment, Gothic, Pointed arch, Scotland, Settlement, Support spread.

### INTRODUCTION

Masonry barrel vaults are an effective type of fire-proof roofing in medieval historic churches, castles or halls, though not as impressive, spatially expressive or prone to experimentation in design as cross vaults. Their form is characterised by the extrusion of a rounded or pointed profile. Often they are very strong as long as they are fully connected to sturdy lateral walls and transverse gables, conditions that limit their spatial expression, as occurred very often with industrial concrete shells in the 1950's [1].

In the Medieval period, most of such vaults are encountered in secular structures like castles and towers in Europe. There is however a characteristic group of pointed barrel vaults in 15<sup>th</sup> century churches and some earlier tower-houses in Scotland [2, 3], which dominate the design of their buildings with a simple behaviour that result from an interaction with their buttresses and support conditions that is more straightforward compared to cross vaults. Most of them are in excellent condition, as a geometric survey showed [4] and the study of their structural performance will reveal more on their margins of strength and their particular construction culture, enhancing our understanding of the experience of their masons and their quest to create new spatial expressions in the periphery of the Gothic architectural world [5]. Moreover, the study will expand our insight into the behaviour of stone barrel vaults, as the Scottish vaults are quite representative of the geometry and support conditions of a broader range.

Up till now, only the historic or architectural evolution of these vaults has been examined [2, 3]. The study will start

\* Address correspondence to this author at the Architectural Technology and Conservation, Edinburgh School of Architecture and Landscape Architecture, University of Edinburgh, 20 Chambers Street, Edinburgh EH1 1JZ, UK; Tel: 0044.141.6502300; E-mail: [d.theodossopoulos@ed.ac.uk](mailto:d.theodossopoulos@ed.ac.uk)

by expanding an earlier review of the geometry [4] and by making a survey of the supports to be analysed, which usually vary from solid continuity along the edge between vault and wall, to interruptions by windows that can be narrow or large traceries framed by pier buttresses.

The performance of these forms is assessed here for the first time and is done by displacement of the supports, evaluating ultimate strength and the evolution of deflections and crack pattern. This is carried out here through an experimental programme, whose innovation is a plain set up that enabled many variations of displacement (symmetric, asymmetric, partial) as also tests to expand the use of the vault through repairs with FRP [6]. The physical models showed clear failure patterns which helped validate numerical simulations (FE and limit state analysis) that ultimately produced deflection and failure patterns under variation of geometric parameters. This study is applied to the Bothwell church outside Glasgow, as it is the earliest of this group of vaults and presents an interesting range of support conditions expressed in the architecture of the building.

## MATERIALS AND METHODOLOGY

### Forms of Scottish Barrel Vaults in the 15C

In particular from elsewhere in Europe, fire-proof stone vaulting developed a simpler configuration of barrel vaults over single naves in Scottish churches in the 15<sup>th</sup> century, in parallel with or even taking over quadripartite cross-vaulting built in the new contemporary burgh churches (St. Gilles in Edinburgh). These vaults mainly roof collegiate churches such as Bothwell (1398), Dunglass (1423), Corstorphine (1429), St. Salvator's in St. Andrews (1450), Seton (1492), or votive churches like Ladykirk (1500), *i.e.* private foundations, distinct from the earlier large scale monasteries. Similar but smaller vaults also characterise votive or burial aisles added to existing churches (Somerville Aisle, at St. Mary's, Carnwath in 1424, Cockburnspath parish church C15, Arbuthnott Chapel from 1505, Wardlaw Vault in Dunfermline in 1617, Dirleton Aisle in 1664, Abercorn in 1727). When referred to their context elsewhere in Europe (*e.g.* intermediate barrel vaults in fortified churches in Navarra, like San Nicolas, 1232 or various vaults in the Cathedral of Girona) their origins to defence structures become stronger.

The study of form from a survey of 5 major case studies [4] shed some light in the designers' choices and their relation to the construction process. The profiles in Corstorphine, Seton, Ladykirk (Fig. 1), Crichton and Dunglass are consistently pointed and there appears to be an underlying scheme of equilateral triangle that defines the overall dimensions of the vault itself (Fig. 2). The comparison of the profiles shows a slow increase in height, and Ladykirk in specific establishes a confident and safe design of pointed shells (6.5m span). Its normalised thrust was calculated as  $0.374wR$  by thrust line analysis of the profile [4, 7] ( $w$  is its weight and  $R$  is the radius of the circular segments is made of), which is relatively low and well contained, and therefore has not caused any defects, in contrast to the visible cracks in Bothwell or the larger vaults of St. Salvator's (9 m span), which had to be taken down in 1773 [8]. In all cases, the construction is solid and of good quality ashlar finish, with almost no deviations of the pointed segments from their original circular profiles. When no deformation is observed in the supports, this quality shows the structural form is neither sensitive to the construction process (whether it progressed from the edge to the crown or end to end).



Fig. (1). The nave, flagstone roof and buttresses of Ladykirk church, Scottish Borders.

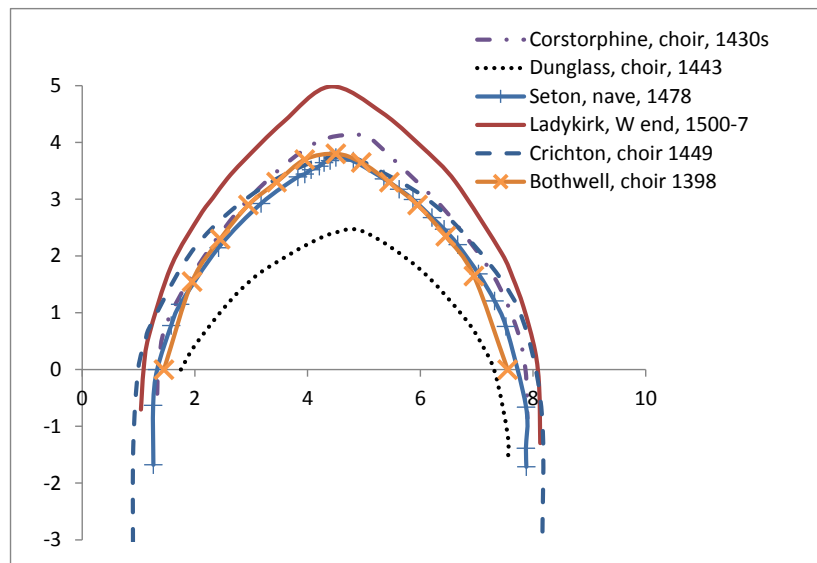


**Fig. (2).** Comparison of representative cross sections between five Scottish case studies of pointed barrel vaults.

The impression of the structures is one of uniformity, maturity and simplicity, comparable to the contemporary context of large stone roofing like the naves of Trinity College and St. Giles in Edinburgh, or St. Mary's in Haddington. These simple forms show Scottish masons were capable of achieving high quality of construction combined with intuitive understanding of the forces (the load path) and strategies for the containment of the resulting thrusts. The thickness of the profile of the vault thins towards the crown and is contained by the gable end, resulting in their behaviour as a rather thick shell. In contrast, in most tower-houses the spandrels are very solid and with very limited openings, producing a 3D structural scheme.

Regarding the use of the key medieval component of ribs, the simplicity of the form does not need the aesthetics of muscular articulation that ribs conferred in earlier/ archaic barrel vaults [9]. Contemporary, more spatially developed examples like the presbytery in Melrose or the almost domical vaults of St. Giles treat ribs as an attached mesh and in Seton or Ladykirk they are used only at the apse, though like a construction element as the vaults' stone plates laid normal to the ribs show. There are however vaults with wide and integrated ribs (Bothwell, Ladykirk), which may demonstrate an awareness of structural concordance with the pier buttresses, beyond a visual bracing and a need to bring a notion of the exterior space into the nave.

### Boundary Conditions and Associated Failure Patterns

The previous study must be completed with a survey of the boundary conditions to frame the performance of these vaults that will be assessed by the models later. The crucial continuity between wall and vault finds various expressions according to the location of openings relative to the springing, from the solid one, with very limited piercing of niches (Dunglass, Corstorphine) to the gradual insertion of traceried windows (Crichton), to such an extent in Bothwell and Ladykirk that the stiff wall plate reduces down to deep pier buttresses. Vaults in tower-houses however, are fully braced by what appears as solid spandrels, which could afford insertion of openings even through the springing line (though limited). The survey and geometric study of the Great Hall (lower vault) in Borthwick Castle, built in Midlothian around 1430 Fig. (3)[10], shows high quality control, especially in the ashlar finish, and successful performance, especially as the tower suffered artillery attack by Cromwell in 1650. The vault dimensions in tower-houses are often larger than in churches, possibly due to the effective bracing (span  $L$  in Borthwick is 7.2 m and span to rise  $L/F= 1.54$ ). Such insertions are not always successful, as the edges in the chamber in Doune Castle show for example.

Containment of the thrust line within masonry is fundamental for the stability of a vault and regarding the support conditions, transverse bracing along the longitudinal edges against the thrust is more important than the integrity of the gables, as indicated at Almond Castle (complete lack of gables) or Dundonald Castle (gable wall eroded around the windows underneath the apex) [11]. The churches are braced with full pier buttresses, sometimes attached at an angle at the corners of the apse, which reduce to half at mid-height. In Ladykirk for example, the piers are 1.2m thick at their

base, while the (rougher) ones at the choir of Dunglass start from 1m. Unique within the period stands Roslin Chapel (1446) with flying buttresses and aisles flanking and bracing the barrel vault of the nave. No empirical rules have been recorded in Scotland, but elsewhere in Spain the late medieval rule of Martinez de Aranda indicates intuitive practice [12]. Using this rule, the effective pier buttresses depth of Seton for example should be ca. 1.5m while the real depth is 5ft or 1.52m [4].

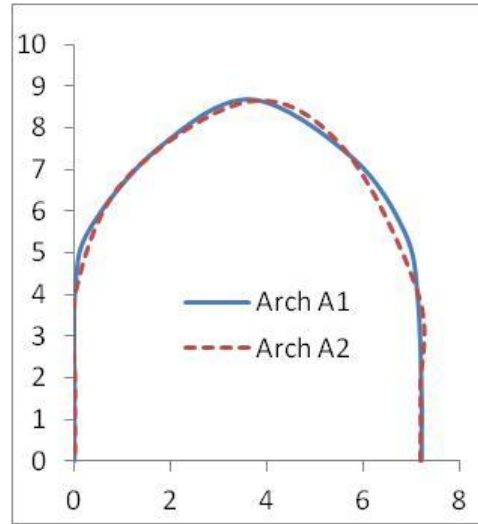
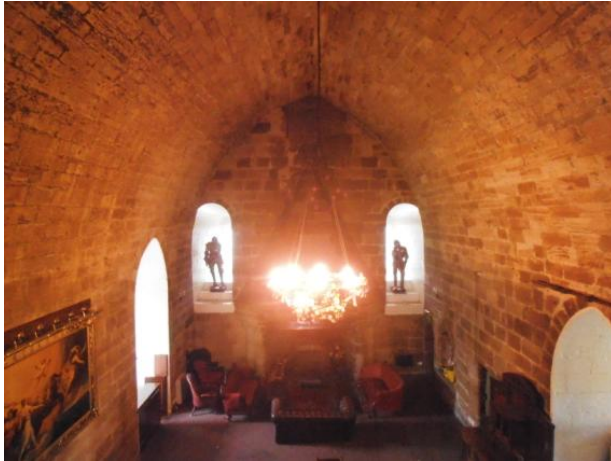


Fig. (3). The Great (Lower) Hall in Borthwick Castle (before refurbishment in 2013) and the geometry of each extreme section (more surveys can be found at [10]).

In this context, the possible failure mechanisms of these vaults depend primarily on the capacity of the buttress & walls system to equilibrate the lower thrust limits and provide enough in-plane stiffness against settlement [12, 13], and secondly on the attachment of the gable end walls. Bothwell Church shows an interesting crack pattern Fig. (4) which is in the course of being repaired. Survey and discussion with John Addison, the project’s structural engineer, showed that the main problem causing the deformations is ground movement due to soft soil under the whole quire (choir). Bracing is stiffer on one end due to the adjacent transept and nave added to the W in 1824, but unfortunately cannot prevent the asymmetric outward spread of the vault at springing level (possibly along the S direction), as becomes evident from the diagonal/ shear cracks (Fig. 4). On the other hand, the stability of the truncated vaults in Dundonald Castle (where the vertex had to be repaired against erosion starting at its ends) and Almond Castle (gable ends lost completely) shows that vaults can develop an essentially linear behaviour as a very wide arch, once it is fixed along the spandrels.

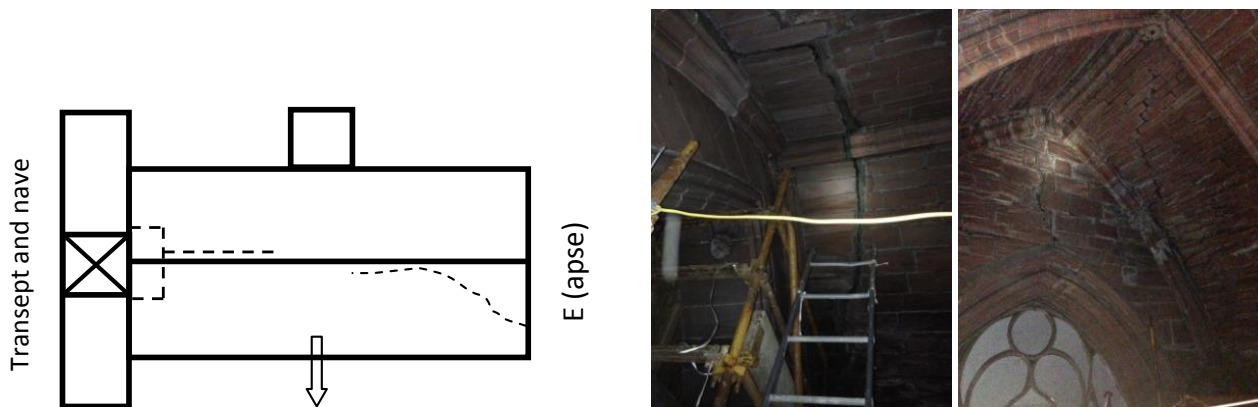
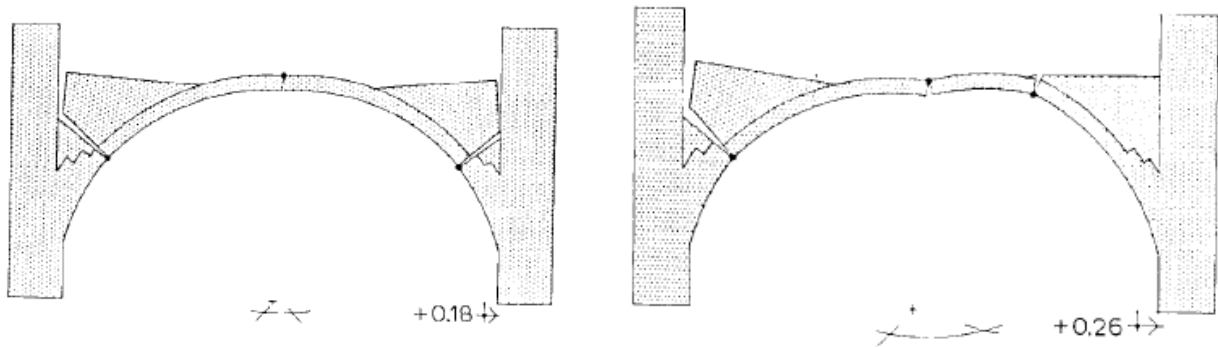


Fig. (4). Cracks pattern due to transverse outward movement drawn at the intrados of the choir in Bothwell church and the cracks next to the transept and apse [6].

### The Effect of the Boundary Conditions

The survey of the support conditions and failure patterns shows the possible alternative structural schemes and therefore redundancies of the system. An adequate approach is then to investigate the effect of asymmetry of lateral movement by a series of tests applying imposed displacement on models of the same geometry. The tests include also the assessment of repairs by FRP, which were planned as an attempt to investigate critical areas of strengthening in real problems like Bothwell. Review of the literature in both fields will highlight failure patterns and displacement limits, as also the effectiveness of repair methods, mainly regarding the location along the geometry and the face of a barrel vault.

A major real case that offers insight to the failure from lateral movement is the lunetted brickwork cross vaults of Cathedral of Sant'Angelo dei Lombardi, which collapsed during the earthquake of Irpinia in S. Italy in 1980. One of the nave vaults was recreated in a full scale model spanning  $L = 7.2\text{m}$  [14] and the effect of the horizontal component of the earthquake was simulated as a static spread of the abutments. The right-hand support was shifted outwards using hydraulic jacks until a 4-hinge failure [15, 16] occurred at  $180\text{ mm}$  ( $1/40$  of  $L$ ) from a combination of three hinge lines at the arch with the spreading support, as shown in Fig. (5). Each part of the vault around the ridge was then repaired with a different technique: on the one section, the cracks were filled with a high strength grout, while in the other the masonry around the crack was rebuilt. The tests show the repairs are effective as the supports could be further displaced to failure at a total of  $260\text{ mm}$  ( $1/28$  of span), *i.e.* 45% more: the grouted portion became rapidly unstable while the rebuilt one developed the same crack pattern as before.



**Fig. (5).** The failure pattern of the vault model in the Cathedral of Sant'Angelo dei Lombardi due to supports spread (left) and the final failure pattern after the repairs (right) [14].

A further group of tests on barrel vaults demonstrated the effect of quarter-span point loading, with restrained supports. Plain tests on ribbed barrel vaults of circular profile spanning  $2.52\text{m}$  [17] established the failure pattern, consisting of a downward longitudinal hinge at the load point and of one of opposite sign, symmetrically located Fig. (6), at a load of  $4.95\text{ kN}$  (producing a  $0.2\text{mm}$  deflection). Afterwards the vault was repaired locally at the faults with FRP, allowing the vault to carry a further load of  $22.5\text{ kN}$ , or 4.5 times higher, reaching a  $0.9\text{mm}$  deflection. When a new vault was reinforced with a regular grid and tested, its strength went beyond  $60\text{kN}$ . In both reinforced cases, the failure occurred at positions similar to the unreinforced one but always around the FRP bands.

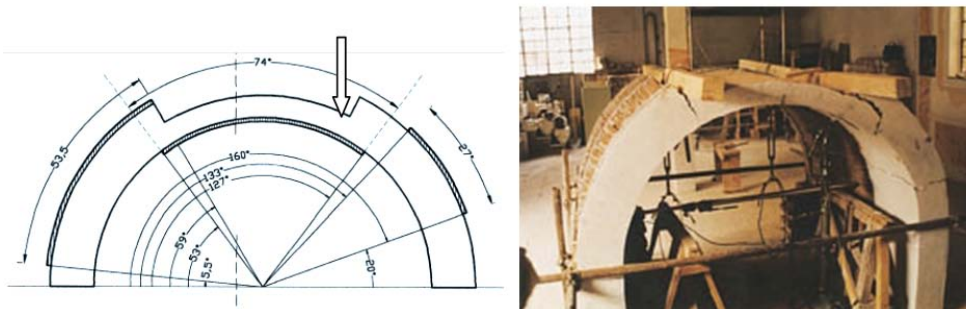


**Fig. (6).** Barrel vault loaded at quarter point (span  $L = 2520\text{ mm}$ : geometry and FRP reinforcement schematic, and failure pattern [17].

Similar tests were carried out by Maria-Rosa Valluzzi *et al.* [18] to study the effect of glass or carbon FRPs on the strength and ductility of thin brickwork vaults, applied on their intrados or extrados. The parameters considered were the ultimate strength of the width of the strips and the bond between the laminate and the masonry. In the case of external strengthening, the line of thrust is expected to fall outside the springings. A brittle mechanism of failure is expected to form due to the sliding between mortar and units, transforming the vault to an isostatic structure consisting of two curved segments that can be effectively strengthened by placing the right amount of fibre along the springing. When strengthened at the intrados, the failure mechanism is ductile and is characterised by the detachment of the fibres locally in the proximity of the loaded section, a problem that can be easier strengthened further.

Other tests on ribbed barrel vaults by Paolo Foraboschi [19] focused on different reinforcement arrangements. The key points that interest this project are that the first group had three  $28^\circ$  long strips attached to the intrados, causing a 4-hinge mechanism at an ultimate load 14.3 times greater than the unreinforced one. The second arrangement had three strips attached to the whole of extrados (outwith the ribs) causing failure by sliding under a load 7.8 times the unreinforced specimen's, while a similar arrangement at the intrados produced ductile failure as in [18] by crushing at considerably greater loads than the plain ones. Finally Laura De Lorenzis *et al.* [20] recommend that FRP reinforcement can substantially reduce the thrust on the piers of an arch (even to complete elimination), when placed spanning an angle centred at the crown along the intrados, or spanning two angles from the abutments towards the haunches (anchored at the abutments) along the extrados.

### Experimental Evaluation of Pointed Barrel Vaults: Set Up of Small-Scale Tests

Most of the tests discussed so far deal with barrel vaults or arches whose failure pattern under certain loads is already established, so they were able to explore geometry or repair parameters. The systematic study of the performance of these Scottish vaults will provide insight on the response of pointed profile forms, and they require failure patterns to pertinent loadings and the effect of repairs to be established first. This will prepare the field for a later parametric study of geometry, loading or arrangement of reinforcement. Moreover, these tests [14, 17 - 20] showed that repairs can be effective but the problem of supports spread or settlement though critical has not been sufficiently studied, so this work will focus on these aspects too.

Scaled models were made of a homogenous semi-brittle material in order to isolate the effect of deformations on the geometric form itself. The prototypes' masonry consists of oblong blocks which make the masonry strongly orthotropic, but this effect will be studied through numerical analysis once the physical models have been validated.

It was decided to find an arch profile from the survey data of 15C Scottish barrel vaults [4] that would represent their geometry and make a synthesis of their proportions (Fig. 2). A scale of 1/15 was chosen for the construction of the models, to enable a reliable repetition of several specimens of the same geometry, at a meaningful consistency and workable dimensions and set up. The representative arch profile chosen for these models has span to rise ratio  $L/F=1.43$ , a springing angle of  $6^\circ$  and a crown angle of  $64^\circ$ , (Fig. 7). The survey showed many vaults cover a length of 12m, so accordingly the models have a length of 0.8m.

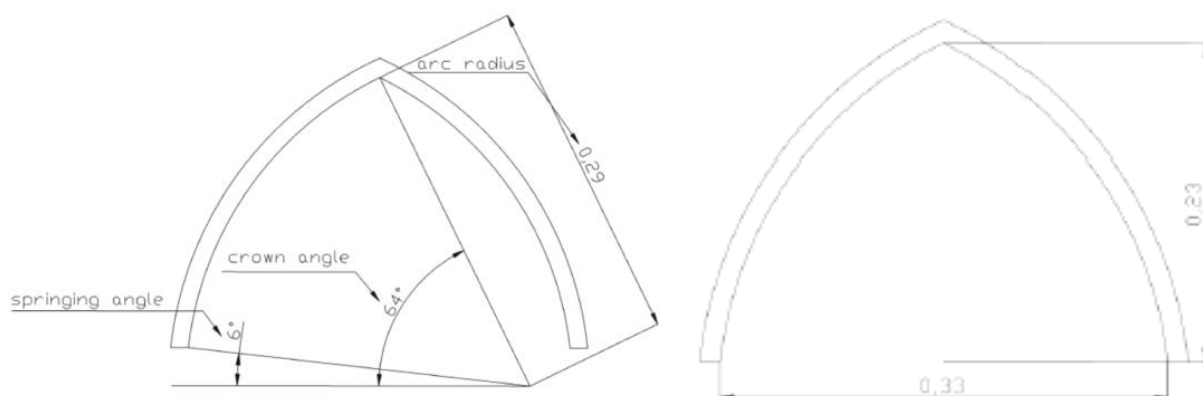
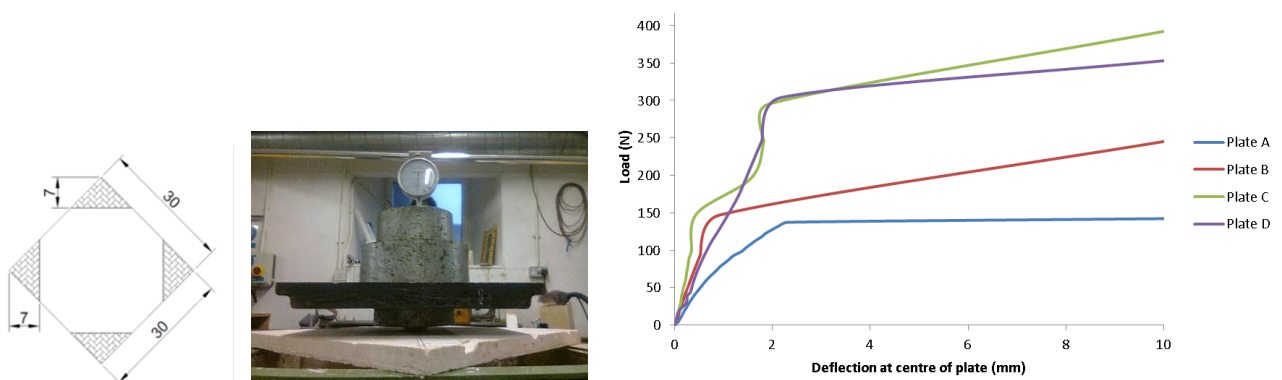


Fig. (7). Generating arch profile used for the models (all dimensions in m).

After a few attempts, a 20mm thick trial vault (BV3) was built with a fine casting plaster to water ratio of 1.375:1 and with two layers of natural scrim fibres in between plaster layers acting as reinforcement. This achieved an increase in the elastic region and produced slower propagation of cracks so that they could be visualised. This model was tested by imposing symmetric spread of the supports, displaying more gradual deformations and slow crack propagation. Nevertheless, in order to decide upon the final thickness and number of layers of scrim fibres to be used, a series of 300x300mm plates of varying thickness and number of layers of scrim fibres were tested at a mid-point load.

Deflections were measured against the applied load and are plotted in Fig. (8): although Plate A appears to reach a plastic “plateau” at a smaller load, the elastic region seems to have a more gentle gradient and the material behaves more closely to a linear elastic perfectly plastic material with much less anomalies than the other plates. Plate A therefore simplified the understanding of the material’s behaviour and was chosen as the material of the model. Combining analysis with Finite Element (that assessed stresses at the plate) with the deflections and load recorded, Young’s modulus for the material was assessed approximately as 525MPa and the yield stress was approximated to 0.63MPa.



**Fig. (8).** Plate tests [6]: set up and deflection results. Plates A, B and C have the same thickness (15 mm) but 2, 4 and 6 layers of vegetable scrim fibres respectively. Plate D has 4 layers reinforcing a 17mm thickness.

Using the pointed arch profile in Fig. (7) a formwork was created and all barrel vault models were cast with two layers of scrim fibres (one layer in each direction in between 2 plaster layers), at a nominal uniform thickness of 15mm. All models and tests are summarised in Table 1, while Table 2 compares the maximum deformations measured at the crown at the point of failure.

**Table 1. Summary of all tests.**

Test	Description	Constraints	Self weight of vault as UDL (kN/m <sup>2</sup> )
BV3	Symmetric spread		0.231
BV4	Asymmetric spread (right-hand side)	Movement of back end restrained with wooden diaphragm plate (“wall”)	0.161
BV5	Central spread	Movement of front and back end restrained with wooden diaphragm plate (“wall”)	0.166
BV5R	Central spread of BV5 after FRP repair	Movement of front and back end restrained with wooden diaphragm plate (“wall”)	0.166
BV6	Asymmetric spread (right-hand side)	Movement of back end restrained with wooden diaphragm plate (“wall”)	0.156
BV6R	Asymmetric spread (right-hand side) of BV6 after FRP repair	Movement of back end restrained with wooden diaphragm plate (“wall”)	0.156
BV7	Asymmetric spread (right-hand side)	Movement of back end restrained with embedded diaphragm plate (“wall”) in plaster	0.154

It was important to be able to impose a spread at the supports of the vault in a smooth and controlled manner without interfering with its response. Metal plates were bent in an angle shape and were attached at the edges of the barrel vault. Turnkeys were fixed on the plates and were used to spread out the supports uniformly if turned at the same time or asymmetrically. Since there were almost no deformations under the maximum uniform dead load that could feasibly be applied, no tests included additional dead loads aside from the self-weight of the vault. The tests confirmed

that the safety of pointed barrel vaults is a matter of geometry, so spreading of the supports provides a much more significant insight on failure.

**Table 2. Summary of maximum crown deformations for all the tests.**

Test	Max (tip) horizontal spread (mm)	Crown	
		x (mm)	y (mm)
<i>Symmetric</i>			
BV3	42	0	-19
<i>Asymmetric</i>			
BV4	49	23	-18
BV6	21	10	-8
BV6R	43	40	-24
BV7	44	1	-43
<i>Symmetric central</i>			
BV5 (mid apex)	16	1	-2
BV5R	20	13	0

The imposed spreads were applied according to meaningful patterns observed in case studies. Symmetric spreads were attempted initially to calibrate the method: some were uniform (BV3) or centrally applied (BV5 and BV5R) and at each case a wooden diaphragm plate at one or the two ends would simulate the rigid constraint of an apse or transept. A lightweight, flat-braid aramid FRP fabric was chosen, with a 45° width of 32 mm, which could easily adapt to an uneven shape [21]. The adhesive was built up of an epoxy laminating resin, a slow hardening agent, and fumed silica thixotropic powder.

Subsequently, as was discussed in the case of Bothwell Parish church, asymmetric displacement of one side of the structure was applied, to represent failure of the lateral walls combined with soil settlement over the years, so tests were set up for spread of the at the right hand side supports (BV4, BV6 and BV6R). BV7 also investigated asymmetric spreading, but a plaster wall of the same material as the vault was fixed to the back end using epoxy.

Dial gauges were set up to measure the spread exactly. The symmetrical spread was applied by turning all the turnkeys on either side of the vault at the same pace. The asymmetric, right-hand-side spread was applied linearly along the edge (Fig. 9): if the back edge was spread by only half a turn, the middle turnkey would have to go through one whole turn and the final turnkey at the front edge by 1.5 turn. This action corresponds approximately to a 2mm spread of the right hand side at the front end, or tip of the edge of the vault.

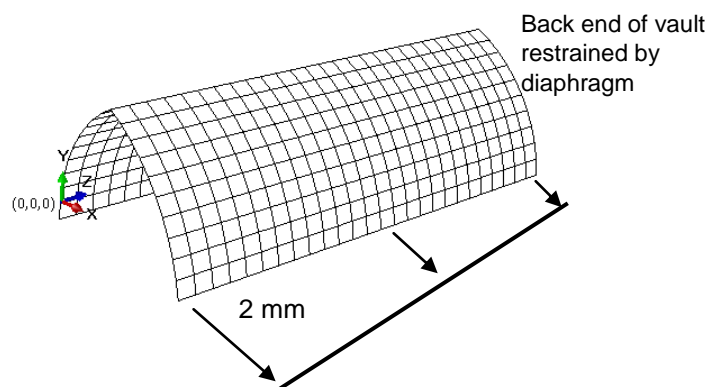
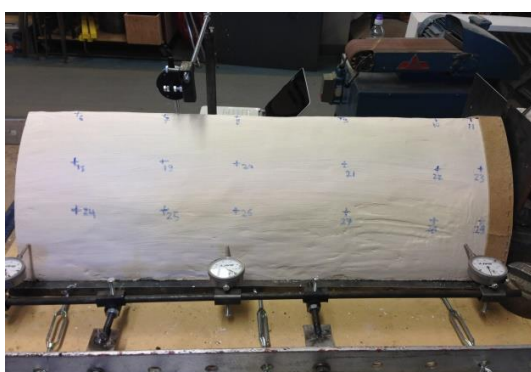


**Fig. (9).** The set up of the tests.

Fig. (10) shows points on the vaults that were monitored using the Leica TPS1200 Total Station. The raw data recorded were translated into Cartesian coordinates using a transformation matrix set up into a spreadsheet by Katherine Primavesi and Jenny Gilbertson [22] so that the front profile lies on the x-y plane and the z-axis is the longitudinal one.

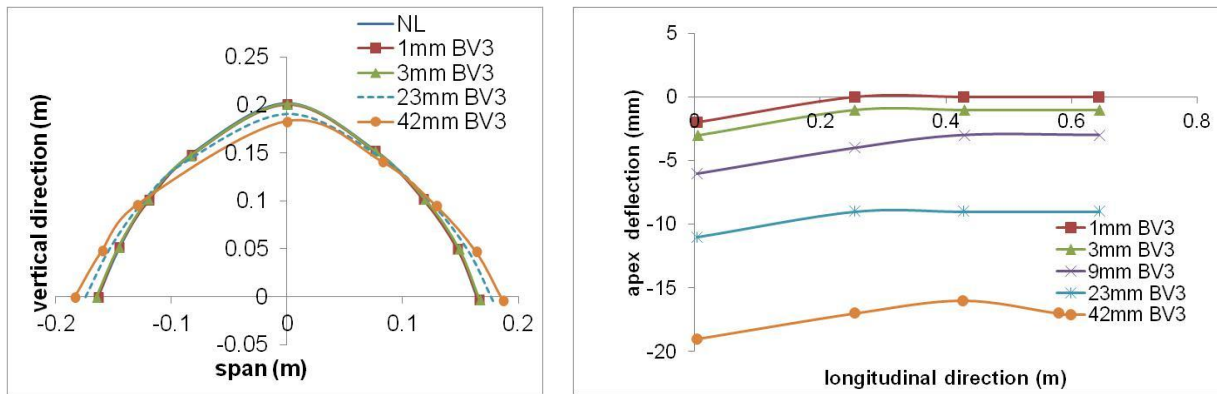


**Fig. (10).** Symmetric spread BV3: the front end (in m) and deflection along the apex (from free front end to the wall at the back).

**RESULTS**

**Test Results**

Tests on vault BV3 imposed a symmetric spread which can be considered as the datum of all the tests (Table 1). The vault could withstand 21mm of spread on each side (total 42mm), causing the apex to deflect by 18mm at the front profile (Fig. 10). These graphs clearly indicate that as the vault is spread outwards, the top portion of the vault deflects downwards whereas the lower portions expand outwards [15, 16]. A crack is formed perfectly along the intrados of the apex, which propagated gradually (Fig. 11), eventually becoming a hinge line and completing the failure pattern as a four-hinge mechanism.



**Fig. (11).** Location of hinge-lines at BV3 (extrados and intrados).

As perfectly symmetric spread of a vault’s springings rarely occurs, the discussion was framed with an asymmetric spread that increases linearly on one edge, while the back end was fixed with a wooden diaphragm wall (test BV4). The right hand side of the front end ultimately undergoes a total outward horizontal displacement of 49 mm (Fig. 12), or 1/7 of span whilst the crown displaces horizontally (x direction) less, 22.7mm (or 1/14 of span) and deflects 22mm. Apex deflection is as expected, the vault deformed almost linearly towards the front end as it was restrained at the back (wall). The horizontal displacement of the apex however occurred at the same rate and the diaphragm wall at the back end seems was not capable of withstanding such spread, contrary to the vertical constraint.

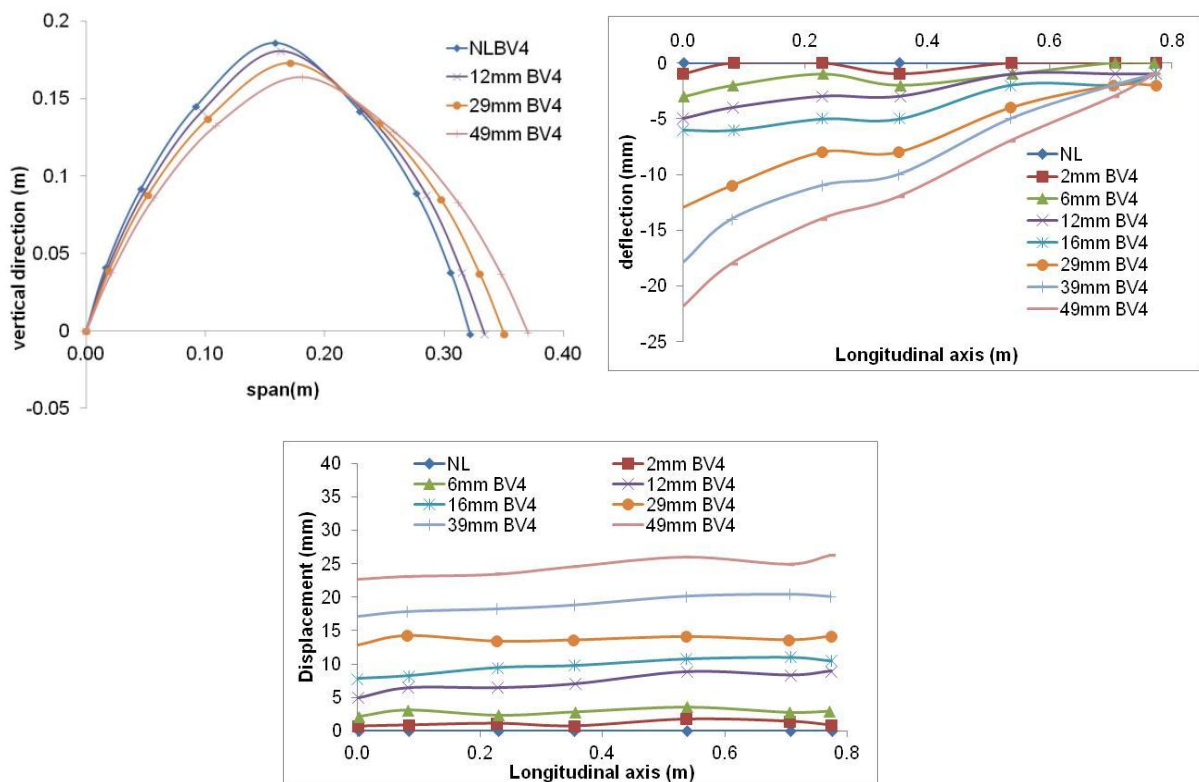


Fig. (12). Test BV4: the front end; deflection and lateral displacement of apex.

Unlike the symmetric spread BV3, a clear hinge line no longer forms throughout the apex or across the length of the vault, instead two cracks appeared at the intrados at the front end of the vault, one at the crown and one on the left hand side (Fig. 13). A crack also formed at the back end of the vault on the extrados. The cracks at the front end eventually spread to the extrados: the crack at the apex propagates more on the extrados whilst the one on the left hand side propagates more on the intrados. The ones at the back end propagate at a similar rate and they almost meet forming a diagonal failure pattern (Fig. 13). This shear type of crack is justified by the differential spread of the front end.

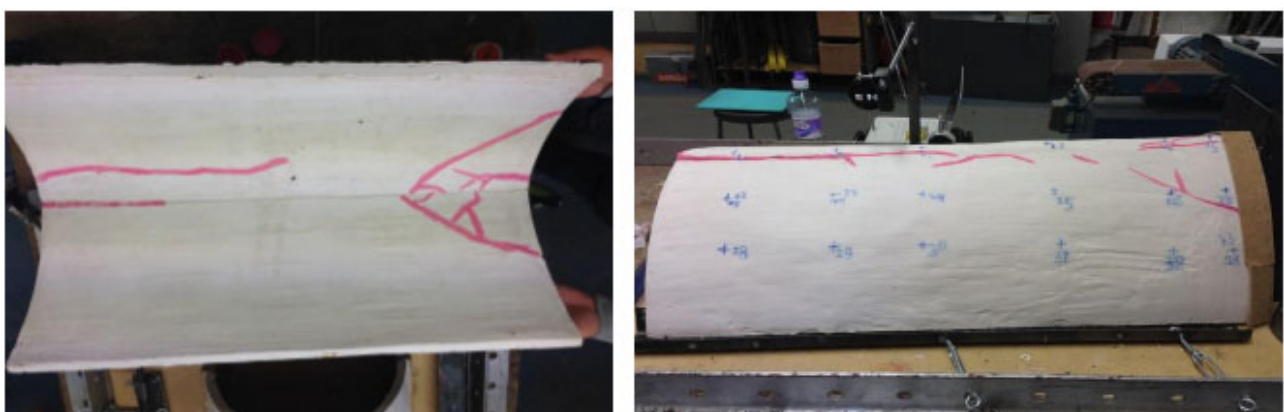


Fig. (13). Test BV4 Crack pattern at intrados and extrados. Maximum movement is applied on the front end (left-hand side in these photos).

**Strength and Repairs**

The ability of repairs to extend the form’s strength to asymmetric spread of one edge (with one wooden diaphragm wall at the back end) spread was assessed against an assumed serviceability limit state. The vault was spread by 9

increments till cracks formed (BV6) before repaired with FRP and was then tested again to failure (BV6R test). The displacement was removed before the repair and the vault almost returned to its original form (vd. profiles NLBV6 and NLB6R in Fig. (15)). The key contribution of the repair is that the vault became reinforced, as the spread at failure went from 22mm (unreinforced) or 1/15 of span to 47mm or 1/7 of span, *i.e.* almost doubled its capacity (Fig. 15).



Fig. (14). Left hand side view in BV6 and right-hand side view of BV6R (the side of displacement application).

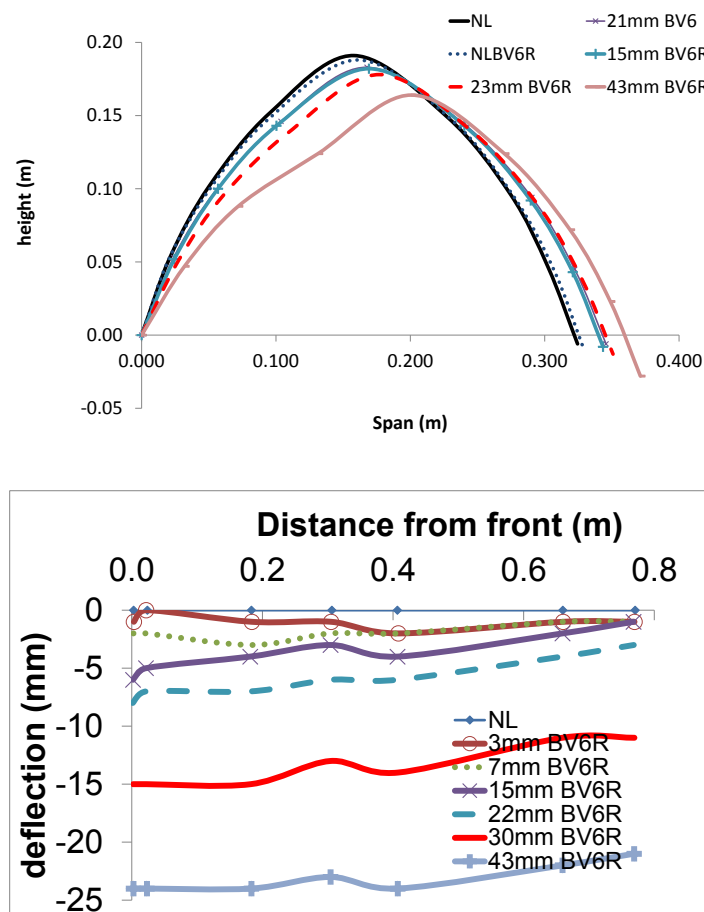


Fig. (15). Front end and deflection of the apex during supports spread, combining tests BV6 and BV6R.

The principal crack at this limit state runs once again diagonally and is clearly appreciated at the extrados, but this time closer to the front end (Fig. 14) when compared to test BV4. At the front end, the crack starts from the left of the crown at a similar location to where the crack started at BV4 and then spreads diagonally but at an earlier stage, in a shear pattern due to the differential spread. The deflections across the vault show some interesting patterns: the

unreinforced vault deflects heavier closer to the front end, but a detachment from the back diaphragm wall also develops, slowly. After reinforcement, the tests BV6R show the vault can take significant more spread, but the vault detaches clearly from the diaphragm and starts behaving like an unsupported barrel vault, as the horizontal displacement of the apex is almost constant across its length (Fig. 15). Most probably, it was the lower parts of the reinforcement, around the spandrels that were more effective in changing this pattern [17].

To assess the strength and contribution of the diaphragm wall, asymmetric spread was once again applied on one side but with a diaphragm wall made of same material as model (test BV7). The first cracks that were produced were visible at the front end around the apex and propagated only a short distance along the apex, deviating towards the right hand side (Fig. 16). As the vault was spread further, two small diagonal cracks became visible at the intrados of the right hand side of the vault. One stems from the bottom of the vault similar to the previous diagonal cracks (BV6). The other crack stems from the back wall, just below mid- height of the vault. This crack proliferates onto the back diaphragm wall where it propagates downwards and a detachment of the plaster wall starts there.



Fig. (16). Crack pattern due to asymmetric spread on a vault model fixed on a diaphragm at the right end made of the same plaster (Test BV7).

Heavy deformation of the front end (Fig. 17) is associated with quite severe cracks and splitting of the vault there around the apex, and this may have been due to insufficient reinforcement (scrim fibres) at this area. This distortion however dies away quickly within the vault, which shows that this fault may be local and the vault have enough redundancies to maintain some geometric integrity. In fact, the rest of the vault spreads outward almost uniformly, except for the diaphragm wall around its crown that does so much less.

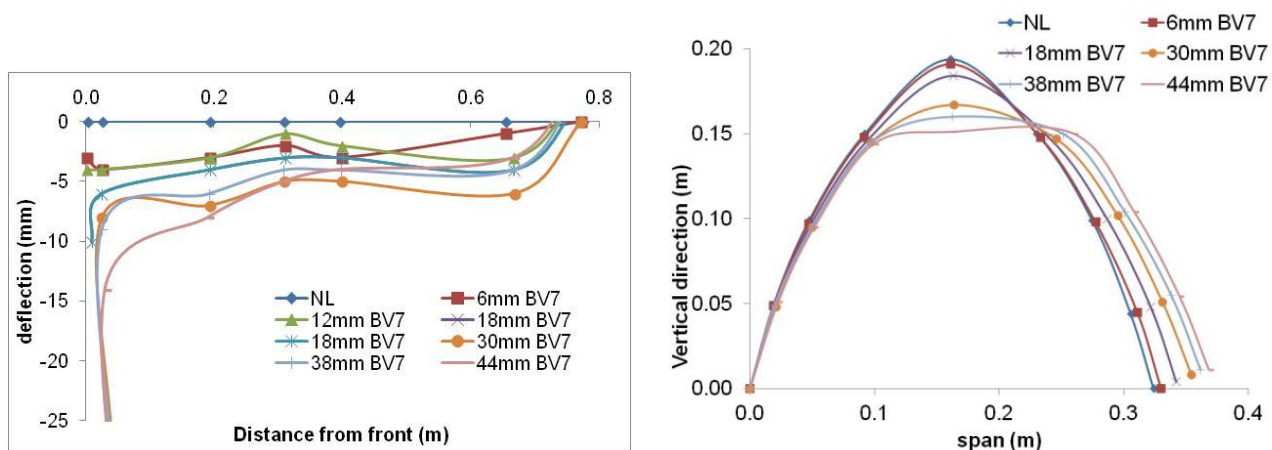
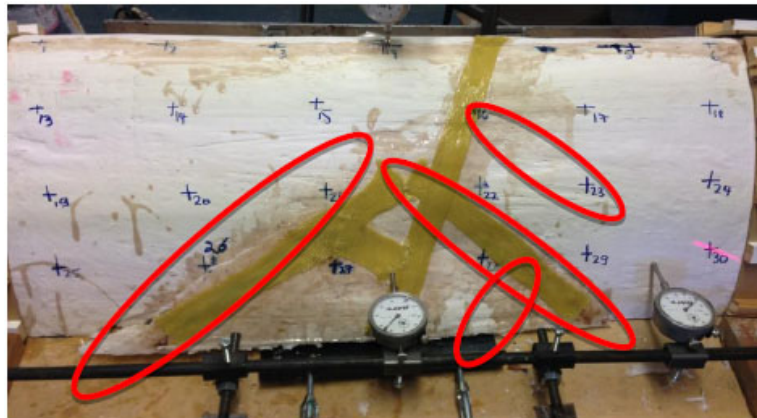


Fig. (17). Test BV7: deflection of the apex plotted against tip displacement and the front end during the asymmetric spread.

The final test was to apply a central symmetric spread only, fixing the vault with two wooden diaphragm walls on either end (test BV5). After the formation of cracks, the vault was repaired as in BV6 (test BV5R). Although the vault was spread uniformly, cracks are formed only on the right hand side of the vault, at  $2 \times 5 \text{ mm} = 10 \text{ mm}$  and the effect of the spread is very localised in that area Fig. (18). Repairs were applied at  $2 \times 8 \text{ mm} = 16 \text{ mm}$  and permitted 10mm more of spread. Two cracks starting from the springing level around the centre of the left hand side of the vault were the first visible extrados cracks. The final cracks at the intrados form on both sides, around the central areas that are spread. As the extrados of the haunches was reinforced, this proved to be effective in resisting better the imposed displacement, similar to the reduction of thrust experienced by De Lorenzis [17].



**Fig. (18).** Centrally-spread vault BV5 after FRP repairs.

**DISCUSSION**

All tests were concluded when the structure was considered to have become unstable or a mechanism and the stages of the impending failure have been recorded. In order to link the observed crack patterns and the deflections measured, the crown deflection was plotted against spread (Fig. 19), showing that apart from the symmetric spread BV3, the asymmetric ones exhibit a non-linear pattern due to the presence of the cracks and the gradual failure, when read with the crack pattern in Fig. (19).

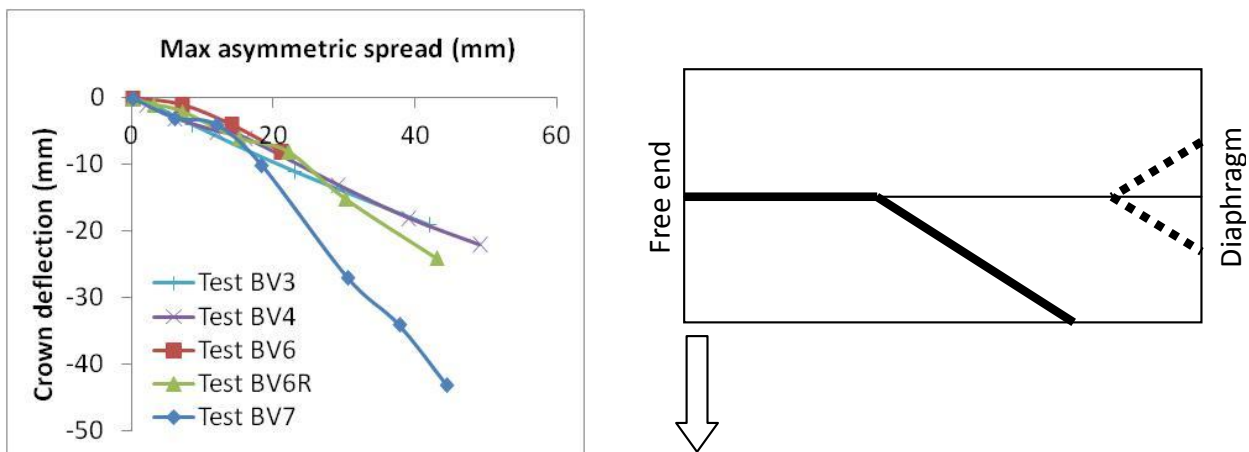


**Fig. (19).** Crown deflection of the tests on plaster models and their FE simulation against tip (maximum) spread, and crack pattern for asymmetric supports spread (continuous line is crack at extrados, dotted is intrados).

Further aspects of the design and performance of this type of barrel vaults can be explored by using analytical methods, once they have been validated with the experimental tests. The Limit State analysis [7, 12, 15] can provide insight to the crack pattern of the models and later to the thrust and stability of the lateral walls of some prototype structures.

Recent research at MIT has produced new computer methods which combine interactive graphic statics, geometry

controlled loads and animated kinematics to allow the application of equilibrium principles in real time instead of performing tedious graphical analysis by hand [23]. A 2D programme called Cabri Geometry II Plus [24] was used to construct the basic arch structure. The analysis incorporates the “lower-bound” or “safe theorem” to produce a line of thrust when the supports are spread, so the vault behaves in a state of minimum thrust [7, 13, 15, 23]. A model of the tests was made: the angle of embrace ( $55^\circ$ ) was divided into 10 parts that looked like voussoirs, with equal surface area and thus equal weights. Then, a macro function helped to find the centroid of each polygon and the line of thrust was constructed, the green line in Fig. (20). The line of thrust touches the boundaries in four places in the case of a pointed arch and hinges form there.

The configuration of the model is changed to mimic an arch being spread; this is done by moving the right abutment outwards first. The rest of the points are then moved accordingly to maintain constant thickness of the arch and the voussoirs. When a 20 mm spread is applied, the line of thrust is not contained on the left-hand side, which results in the formation of two hinges on either side of the crown and two more at the intrados of the abutments where two hinges (Fig. 20). This results in failure of the 2D arch and a capacity of 20 mm spread (1/16 of span).

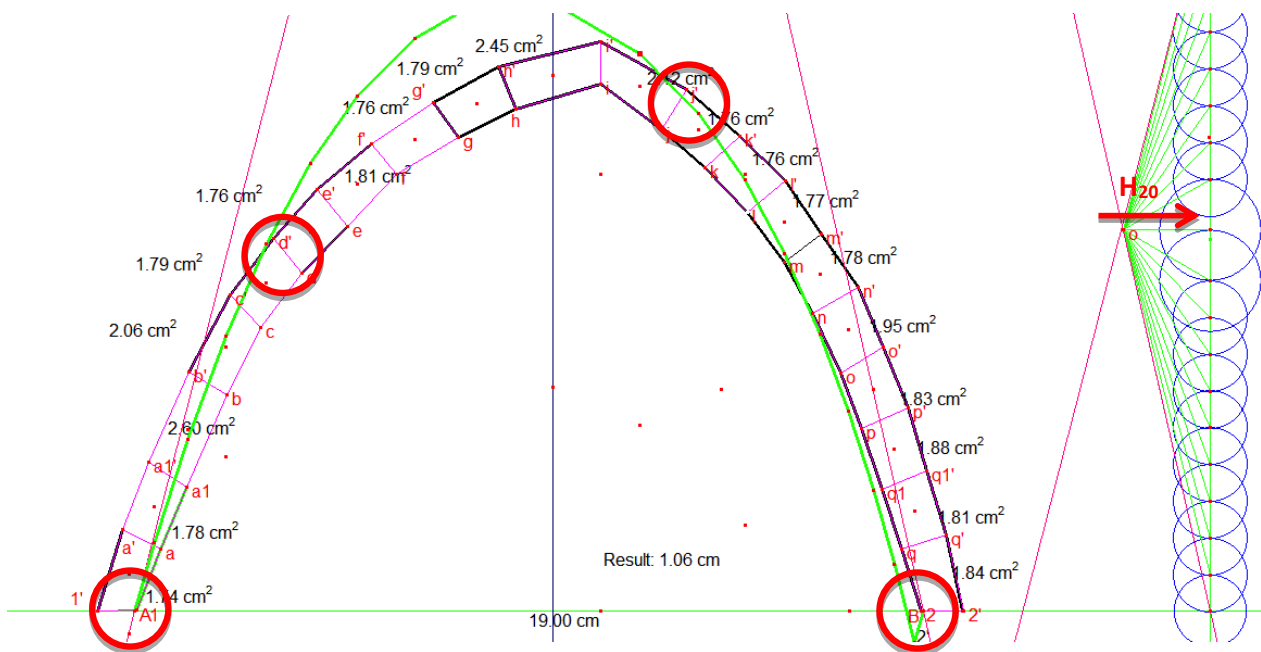


**Fig. (20).** Simulation of asymmetric spread of the right-hand support, in an arch with the same dimensions as a cross section of the tested vaults. The capacity of the arch is surpassed at a 20 mm spread, where 4 hinges form.

This graphic-statics analysis is predominantly a two-dimensional approach of “slicing” the 3D structure into 2D sections and confirms when some of the cracks form Figs. (11, 13, 14, 16, 19), but not the failure of the entire vault. This method was further developed into Thrust-Network Analysis, a three-dimensional computational method which produces lower-bound solutions of masonry vaults with complex geometries [23], and it would be worthy investigating its application at a further stage. A continuous shell analysis is a more straightforward option to assess the load-sharing and the tests were used to validate a homogeneous FE macro-model (Fig. 17). This would then serve to explore the strength of key examples of barrel vaults to supports spread and the effect of some design aspects.

A FE model of the tested forms was analysed in the program ABAQUS [25] as a homogeneous, isotropic shell using S4R5 type elements to represent the thin plaster models. To maintain insight to the behaviour resulting from the tests, a linear elastic model with perfect plasticity defined by a single yield stress (0.63 MPa) was used for the material behaviour and failure was modelled with a smeared crack approach using a failure criterion defined by this yield stress. In order to create elements of equal length, a MATLAB script was created which used the equation of a segment of the circle that defined the arch profile. The plate tests (Fig. 8) were also simulated in FE to calibrate the material model, showing satisfactory correlation with the failure process and formation of the plastic plateau.

The discussion of the tests showed that plotting the deflections of the crown of the front end is quite representative of the behaviour of the model, so it will be used to validate the FE model. Regarding asymmetric movement, the FE model was spread linearly along the right-hand side edge only. The correlation of the deflections of the front end crown (Fig. 21) is satisfactory, especially for tests BV4, BV6 and initial stages of BV6R, except for the case of BV7 where as was mentioned heavy crack and separation occurred at that point (Fig. 17), possibly due to a local material fault as was discussed earlier. The plot of the plastic hoop stresses S11 at failure (Fig. 21), which indicate the smeared cracks, also correlates with the crack pattern observed in the asymmetric spread tests, which develops after a tip spread of 11mm (or 1/30 of span) and can be considered as the yield point of the model. The differences in deflection after that point can be attributed to the physical split of the tests models, which the continuous shell FE model cannot reproduce to the same extent. Similarly, the difference with test BV6R can be attributed to deformations that may have been embedded after the repairs, causing higher deformations.

Variation of the diaphragm wall stiffness or even its removal increased slightly the deflections. This together with the close values of the asymmetric tests (Fig. 21) confirms that once cracks have formed, especially along the apex, the failure of the vault is in essence geometric. The shear cracks along the middle of the vault are due to the continuity of the vault, and therefore can only be captured by 3D limit-state tools.

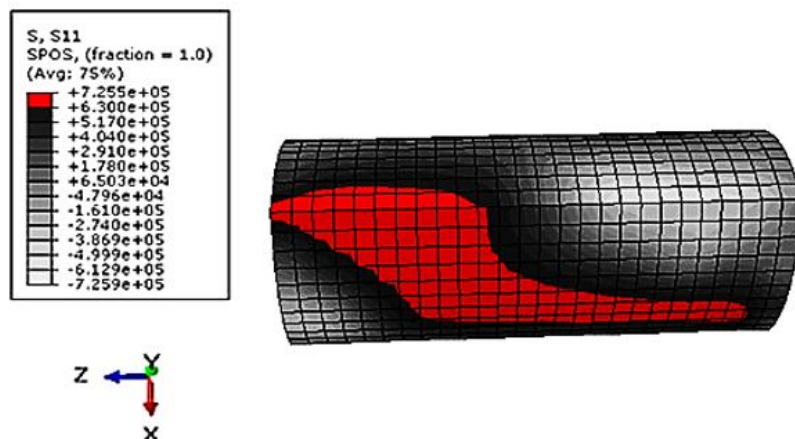


**Fig. (21).** Hoop stresses at the intrados of the FE model at failure from asymmetric support movement. The light (red) areas indicate plastic failure and the spread of (smeared) cracks.

**Application to Bothwell Church**

The FE model can be used now to examine the process of lateral deformation in real case studies, together with other actions like settlement. The form of the barrel vault in Bothwell will be used Figs. (2, 4) and the effect of these actions on other vaults of this type will be left for further investigation. A uniform thickness of 0.3m was assumed for the vault and no consideration was made for the weight of the flagstone roof, a spandrel fill or even the presence of diaphragms possibly in line with the embedded ribs, as these can be part of further parametric study which outweighs the scope of this paper. The entire length of the nave was modelled (15.8m), but only above the springings, *i.e.* ignoring the effect of the transepts, which can be positive as bracing against lateral movement or adversary as interruption of the bracing by the wall stiffness against settlement. The one end was considered as free and two options were taken for the other end, free or pinned (diaphragm) to frame the possible effect of the apse.

**Table 3. Material properties of the FE model for Bothwell [26].**

Material properties	Parallel to bed joint (long. direction)	Normal to bed joint (hoop direction)
Elasticity modulus, E (N/mm <sup>2</sup> )	4200	670
Bending strength, F <sub>u</sub> (N/mm <sup>2</sup> )	0.98	0.32

Apart from the scale, a key difference with the model is the orthotropic nature of the masonry (Fig. 4), therefore a method used earlier to study the failure of Holyrood Abbey church [26] will be adapted here, using the same material properties here as well (Table 3). The orthotropic elastic modulus and bending strength were combined into a simplified version of a biaxial brittle failure criterion that controls the smeared crack approach, but the principles remain the same:

once the strength in one direction is exceeded, the corresponding elastic modulus  $E$  is dropped to almost 0 (a smeared crack). Failure at a node occurs when the strongest direction (longitudinal in this case) has cracked following the weaker direction (along the hoop here). No biaxial combination is made here and the USDFLD type subroutine of Abaqus [25] is used to control the process and highlight the points of failure. These points are then mapped and failure occurs when enough yield lines have formed to transform the structure to a mechanism, rather than when the analysis has been concluded.

The asymmetric support movement presents some interesting trends. When a diaphragm is considered at the transept and the apse is free, the principal yield line forms slowly at 0.34m of spread (or 1/18 of span 6.1m), producing a crown deflection of 14mm (Fig. 22). The process is slower however when both ends are free: the first cracks appear at 0.22m along the apex causing a larger deflection (76mm) and then they spread slowly to the centre, when they form a continuous yield line that marks failure at 0.88m (1/7 of span). This impression of higher redundancy of the free vault is false though as the pinned vault does not deform as heavily, but on the other hand the free vault gives ample warning of the incoming failure, even though with heavier and possibly unrecoverable deformations.

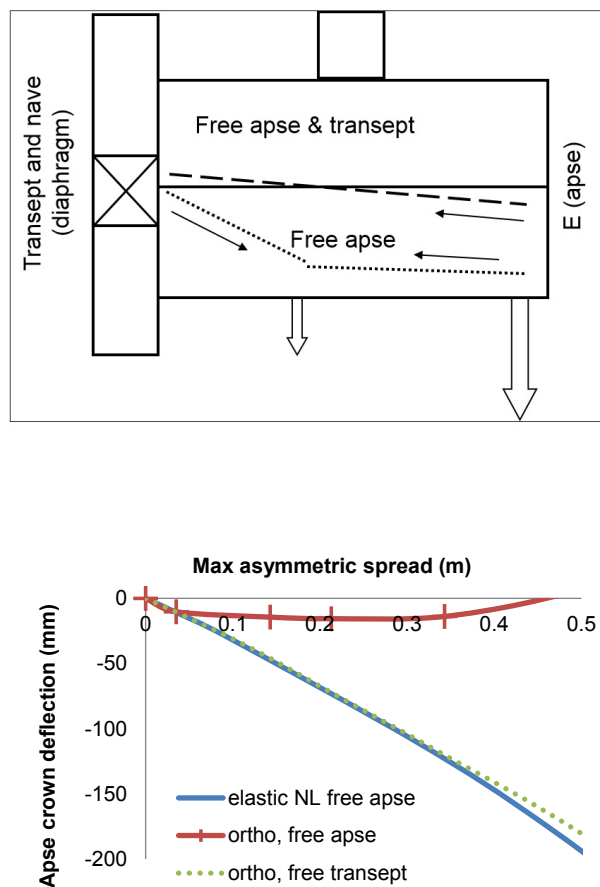


**Fig. (22).** Failure mechanism and crown deflection against tip (maximum) asymmetric horizontal movement of the supports in the Bothwell FE model for the two options of support conditions, showing propagation of failure.

A similar observation on the role of the supports can be made for linear settlement applied along one edge only of the vault (Fig. 23). For the vault with diaphragm at the transept and free apse, the yield line forms slowly at 0.62m max settlement (deflection -156mm), while at the one with both free ends the yield line forms too slowly to be meaningful, probably due to the immediate bracing effect of the applied horizontal constraint along the edge.

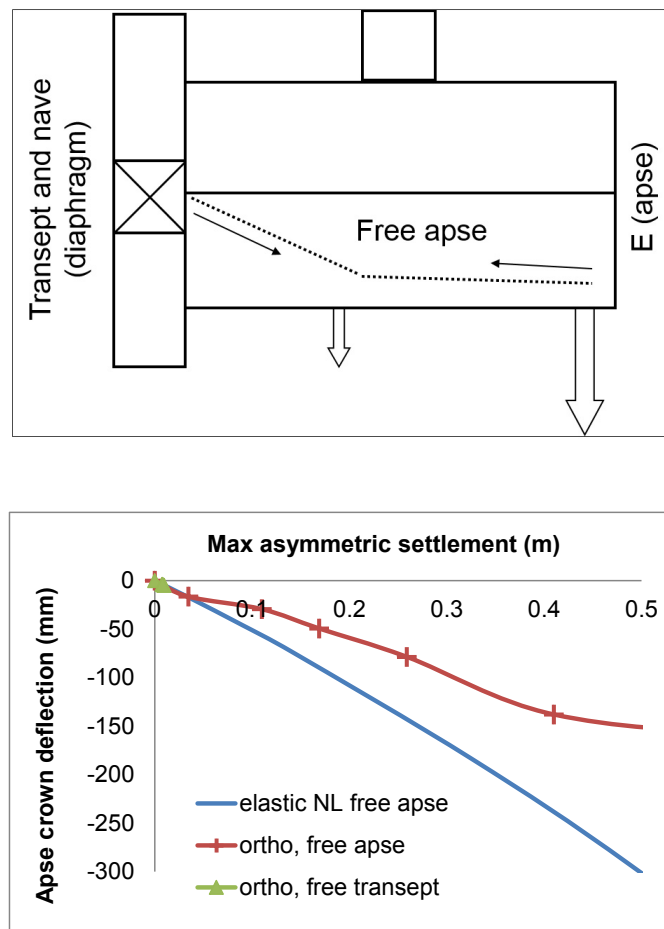


**Fig. (23).** Failure mechanism and crown deflection for asymmetric settlement of the supports in the Bothwell FE model, for the support conditions considered here, showing the direction of the spread of failure.

The orthotropic masonry increases the vault’s strength when the resulting deflections are compared to those of the isotropic model (Figs. 22, 23), as the stronger longitudinal direction resists the spread of failure. The supports displacement also compares well in terms of magnitude with those recorded for other gothic vaults [27], which tend to fail later however due to the stiffening effect of the transverse vaults (assuming that the construction quality and continuity of the vault along the ribs is good). Overall, the FE model is in good agreement with the deformation of the church and offers more insight on the sensitivity of the vault to the support conditions, as the combination of settlement and displacement can produce a pattern similar to Fig. (4)

**CONCLUSION**

This study provides insight to the structural performance of Scottish barrel vaults of the 15<sup>th</sup> century, while at the same time examines the strength of vaults to imposed deformations, beyond the usual tests dealing with point loads, which are the conditions found in bridges or soffits. Figs. (19, 22, 23) established failure patterns and assessed the effect of repairs, preparing effectively the field for a parametric study of geometry, loading or arrangement of reinforcement.

The simulation of the effect of boundary conditions like asymmetric spread or settlement of one edge shows that cracks propagate rapidly and cause early failure in the form of diagonal crack patterns across the vault. Bracing with gables (diaphragms) provided more stiff areas but also a sharper failure, as the free vault continued to deform, possibly however beyond repair. Compared to tests under point loads, the deformation under these conditions is much more severe and occurs rapidly. The insight also frames the full scale tests by Ortolani [13] under symmetric uniform spread, where failure by four hinge lines occurred at 180 mm spread (1/40 of L), *versus* the effect of asymmetric spread that caused the collapse of the FE model of Bothwell at 883 mm (1/7 of L). Unfortunately those tests [13] did not record deflections, but if they are used as a guidance for the performance of these forms, then the isotropic studies show that

failure eventually develops as geometric instability (Fig. 19), and the orthotropic masonry bond in these vaults shift the patterns significantly and increase their strength (Figs. 22, 23) as parts of the cracks spread slower, producing instability of the entire vault later.

## CONFLICT OF INTEREST

The authors confirm that this article content has no conflict of interest.

## ACKNOWLEDGEMENTS

Malcolm Cruickshank and Paul Diamond, technicians of the Architecture workshop in Minto House have offered fundamental support to the tests. Dr. Tim Stratford at the School of Engineering gave valuable guidance to the application of FRP. The communities in the churches, especially Christine Mill at Corstorphine, Henry Duncan at Crichton, Nigel Bruce at Dirleton, Rev. Alan Cartwright at Ladykirk and Gail Wilson at Borthwick Castle have to be thanked for essential access to their monuments, as also Historic Scotland for access to Seton and Dunglass. Roger Taylor and John Addison, respectively the architect and structural engineer for Bothwell are also warmly thanked for the insight to the problems of the church, as also Bob Hislop for information on the restoration of Dundonald Castle he carried out when working at Historic Scotland.

## REFERENCES

- [1] A. Chronowitz, *The Design of Shells: A Practical Approach*, Crosby Lockwood: London, 1960.
- [2] R. Fawcett, *The Architecture of the Scottish Medieval Church 1100-1560*, Yale University Press: London, 2011.
- [3] R. Fawcett, "Barrel-vaulted churches in late medieval Scotland", In: C. Stevenson, and T.A. Heslop, Eds., *Architecture and Interpretation. Essays for Eric Fernie*, Boydell & Brewer: Martlesham, 2012.
- [4] D. Theodossopoulos, "Stone barrel vaulting in late medieval churches in Scotland", In: *Proceedings of the First Construction History Society Conference*, Cambridge, July 11-12, 2014, pp. 1-14.
- [5] M.T. Davis, "Sic et non: recent trends in the study of gothic ecclesiastical architecture", *Jnl. Soc. Arch. Historians*, vol. 58, no. 3, pp. 414-423, 1999.  
[<http://dx.doi.org/10.2307/991535>]
- [6] L. Akl, and N.C. Makoond, *"The Failure of Gothic Pointed Arched Barrel Vaults"*, Dissertation for the degree of BEng(Hons) in Civil Engineering, University of Edinburgh, UK, May 2014.
- [7] J. Heyman, *The Stone Skeleton*, Cambridge University Press: Cambridge, 1995.  
[<http://dx.doi.org/10.1017/CBO9781107050310>]
- [8] R.G. Cant, *The College of St. Salvator*, Oliver and Boyd: Edinburgh, 1950.
- [9] L.R. Hoey, "A problem in Romanesque aesthetics: the articulation of groin and early rib vaults in the larger churches of England and Normandy", *Gesta*, vol. 35, no. 2, pp. 156-176, 1996.  
[<http://dx.doi.org/10.2307/767180>]
- [10] Entry for Borthwick Castle at the CANMORE database of the Royal Commission for Ancient and Historic Monuments in Scotland (RCAHMS). Available at: <http://canmore.rcahms.gov.uk/en/site/53239/details/borthwick+castle/> [Accessed April 2014].
- [11] *Interview with Bob Hislop, Architect with Historic Scotland and Restorer of Dundonald Castle*, December 2014.
- [12] S. Huerta, "Geometry and equilibrium: The gothic theory of structural design", *Struct. Eng.*, vol. 84, no. 2, pp. 23-28, 2006.
- [13] C. Blasi, and P. Foraboschi, "Analytical approach to collapse mechanisms of circular masonry arch", *J Struct Eng (ASCE)*, vol. 120, no. 8, pp. 2288-2308, 1994.
- [14] F. Ortolani, "Effetti del terremoto sulle strutture laterizie voltate", In: *Palladio, Rivista di Storia dell'Architettura e Restauro n. s., anno I, No. 2*, Rome, Italy, 1988.
- [15] J. Ochsendorf, "The masonry arch on spreading supports. The structural engineer", *Ins. Stru. Eng. London*, vol. 84, no. 2, pp. 29-36, 2006.
- [16] P. Foraboschi, "Resisting system and failure modes of masonry domes", *Eng. Fail. Anal.*, vol. 44, pp. 315-337, 2014.  
[<http://dx.doi.org/10.1016/j.engfailanal.2014.05.005>]
- [17] R. Di Marco, P. Faccio, P. Foraboschi, and E. Siviero, "Volte in muratura rinforzate con FRP", *Costruire in Laterizio*, vol. 69, pp. 66-71, 1999.
- [18] M.R. Valluzzi, M. Valdemarca, and C. Modena, "Behaviour of brick masonry vaults strengthened by FRP laminates", *J. Compos. Constr.*, pp. 163-169, 2001.  
[[http://dx.doi.org/10.1061/\(ASCE\)1090-0268\(2001\)5:3\(163\)](http://dx.doi.org/10.1061/(ASCE)1090-0268(2001)5:3(163))]
- [19] P. Foraboschi, "Strengthening of masonry arches with fiber-reinforced polymer strips", *J. Compos. Constr.*, vol. 8, no. 3, pp. 191-202, 2004.  
[[http://dx.doi.org/10.1061/\(ASCE\)1090-0268\(2004\)8:3\(191\)](http://dx.doi.org/10.1061/(ASCE)1090-0268(2004)8:3(191))]

- [20] L. De Lorenzis, R. Dimitri, and A. La Tegola, "Reduction of the lateral thrust of masonry arches and vaults with FRP composites", *Construct. Build. Mater.*, vol. 21, pp. 1415-1430, 2007.  
[<http://dx.doi.org/10.1016/j.conbuildmat.2006.07.009>]
- [21] D. Theodossopoulos, J. Sanderson, and M. Scott, "Strengthening masonry cross vaults damaged by geometric instability", *Key Eng. Mater.*, vol. 624, pp. 635-643, 2015.  
[<http://dx.doi.org/10.4028/www.scientific.net/KEM.624.635>]
- [22] K. Primavesi, and J. Gilbertson, "*The Safety of Iron Age Brochs*", Dissertation for the Degree of MEng(Hons) in Civil & Environmental Engineering, University of Edinburgh, UK, May 2013.
- [23] P. Block, T. Ciblac, and J. Ochsendorf, "Real-time limit analysis of vaulted masonry buildings", *Comput. Struct.*, vol. 84, no. 29, pp. 1841-1852, 2006.  
[<http://dx.doi.org/10.1016/j.compstruc.2006.08.002>]
- [24] "*Cabri Geometry II Plus*" Available at: <http://www.cabri.com> [Accessed December 2014].
- [25] "*Abaqus version 6.10, Finite Element Analysis software by Simulia, Dassault Systemes*" 2015. Available at: <http://www.3ds.com/products-services/simulia/products/abaqus/>
- [26] D. Theodossopoulos, B.P. Sinha, and A.S. Usmani, "Case study of the failure of a cross vault: church of holyrood abbey", *J. Archit. Eng.*, vol. 9, no. 3, pp. 109-117, 2003.  
[[http://dx.doi.org/10.1061/\(ASCE\)1076-0431\(2003\)9:3\(109\)](http://dx.doi.org/10.1061/(ASCE)1076-0431(2003)9:3(109))]
- [27] D. Theodossopoulos, and B.P. Sinha, "Structural safety and failure modes in gothic vaulting systems", In: *Proceedings of the 8<sup>th</sup> International Seminar on Structural Masonry*, Istanbul, November 2008.

---

© Theodossopoulos *et al.*; Licensee *Bentham Open*.

This is an open access article licensed under the terms of the Creative Commons Attribution-Non-Commercial 4.0 International Public License (CC BY-NC 4.0) (<https://creativecommons.org/licenses/by-nc/4.0/legalcode>), which permits unrestricted, non-commercial use, distribution and reproduction in any medium, provided the work is properly cited.